Research Article Vol. 32, No. 3 / 29 Jan 2024 / Optics Express 4327
Optics EXPRESS

Chiral optical solitons in an electrically active multiferroic guiding structure

VAKHTANG JANDIERI,[1] RAMAZ KHOMERIKI,[2,*] KOKI WATANABE,[3] DANIEL ERNI,[1] DOUGLAS H. WERNER,[4] AND JAMAL BERAKDAR[5]

[1]*General and Theoretical Electrical Engineering (ATE), Faculty of Engineering, University of Duisburg-Essen and CENIDE —Center for Nanointegration Duisburg-Essen, D-47048 Duisburg, Germany*
[2]*Physics Department, Tbilisi State University, 3 Chavchavadze, 0128 Tbilisi, Georgia*
[3]*Department of Information and Communication Engineering, Fukuoka Institute of Technology, 3-30-1 Wajirohigashi, Higashi-ku, Fukuoka 811-0295, Japan*
[4]*Department of Electrical Engineering, The Pennsylvania State University, University Park, PA 16802, USA*
[5]*Institut für Physik, Martin-Luther-Universität, Halle-Wittenberg, D-06099 Halle/Saale, Germany*
[*]*ramaz.khomeriki@tsu.ge*

Abstract: A stack of a dielectric planar waveguide with a Kerr-type nonlinearity, sandwiched between two oxide-based helical multiferroic layers is shown to support electrically-controlled chiral solitons. These findings follow from analytical and full numerical simulations. The analytical scheme delivers explicit material parameters for the guided mode soliton and unveils how the soliton propagation characteristics are controlled by tuning the multiferroic helicity and amplitude of the injected electromagnetic wave. Silicon and CS_2 are considered as the optical media in the guiding region enclosed by the multiferroic slabs. CS_2 has very similar nonlinearity characteristics to silicon but in the linear regime it exhibits a smaller refractive index in the THz frequency range. The scattering simulations are performed using our developed numerical code based on the rigorous coupled wave method and the results for the dispersion curve for the guided mode agree very well with the analytical formula that we derive in this work. The results demonstrate a case of nonlinear pulse generation with field-controlled, nontrivial topological properties.

1. Introduction

Optical nonlinearities are the basis for numerous phenomena and functional photonic devices such as higher harmonic generation, optical amplifiers, switches and modulators. An excellent, frequently used optical medium is silicon [1] - having a high nonlinear index with extremely low losses and operating mainly in the infrared range of the light spectrum. In the THz range, plenty of candidates with high Kerr-type nonlinearity are available [2]. However, these materials are conventionally isotropic and do not support the generation of nontrivial topological effects. A way to remedy this situation is the integration of Kerr-type nonlinear materials within an optically highly anisotropic medium. Here, we will use the anistoropy provided by oxide-based multiferroic layers which are known to possess tunable topological properties.

In [3] we have shown that a dielectric slab interfaced with top and bottom dielectric multiferroic oxide layers with nonzero ground-state spin helicity can selectively trap certain chiral modes [4–8], whereas other modes leak out from the guiding region. Therefore, for a fixed value of the radiation frequency only a single mode with a particular propagation constant survives. The considered multiferroic material hosts a spin-current-driven electric polarization to which an external static electric field can couple changing in turn spin ordering (and in particular the spin chirality) and hence, the propagation constant and the photonic chirality density of the modes. In this paper we consider the nonlinear photonic properties of this chiral photonic/spintronic

#507216 https://doi.org/10.1364/OE.507216
Journal © 2024 Received 28 Sep 2023; revised 25 Nov 2023; accepted 28 Nov 2023; published 25 Jan 2024

Optics EXPRESS

device. Our goal is the formation of a guided mode soliton and its control by properly adjusting the radiation frequency, injected signal amplitude, and the multiferroic spin helicity index.

A suitable electrically tunable material class are dielectric multiferroic oxides with spin-current induced ferroelectricity such as RMn_2O_5 (R=Y,Ho,Bi) [9], $DyMnO_3$ [10], or $TbMnO_3$. In the helical phase, the ferroelectric polarization $\mathbf{P}_0$ is related to the helical spin order (due to the inverse Dzyaloshinskii-Moriya interaction) as indicated by the well-defined value of the vector spin chirality along the x-axis, $\kappa_{j,x} = (\mathbf{S}_j \times \mathbf{S}_{j+1})_x$ (where $\mathbf{S}_j$ describes the spin on site j, as shown in Fig. 1(a)). A collinear spin order implies $\kappa_{j,x} = 0$ and thus a vanishing $\mathbf{P}_0$, and vice versa. This phenomenon is caused by intrinsic interactions and their interplay such as the spin-orbit coupling, crystal field effects, and electronic correlations [11–14]. Of importance here is the observation that an applied static electric field $\mathbf{E}_0$ changes the energy and the phase of the systems by the amount $-\mathbf{E}_0 \cdot \mathbf{P}_0$ and can drive the system from the chiral phase to the collinear one [11]. Therefore, spin-dependent scattering of electromagnetic waves [15] can be tuned by electric means. On the other hand, the contribution of the emergent polarization to the total free energy is marginal (due to weakness of magneto-electric coupling), so the main effect of multiferroicity is the change in the spin ordering. The dielectric polarization reads:

$$\mathbf{P} = \epsilon_0 \mathbf{E} \left(n_0^2(y) - 1 + c n_0^2(y) \epsilon_0 n_2(y) |\mathbf{E}|^2 \right) \tag{1}$$

where ϵ_0 is the permittivity of free space, $\mathbf{E}$ is the time varying electric field vector of the electromagnetic radiation, the Kerr-type nonlinear refractive index is represented as $n = n_0 + n_2 I$ with the nonlinear coefficient n_2, and the optical wave intensity $I = c n_0(y) \epsilon_0 |\mathbf{E}|^2/2$. Here, the linear refractive index $n_0(y)$ varies along the y-axis. Inside the nonlinear medium the refractive index is constant as $n_0(y) = n_0$. The refractive index of the multiferroics is $n_0(y) = n_0'$. The nonlinear coefficient $n_2(y)$ is taken as nonzero only inside the nonlinear material. Our goal is to quantify whether a nonlinear region (with a thickness w) sandwiched between two helical multiferroic layers (cf. Fig. 1(a)) would support propagation of a chiral envelope soliton and determine the dependence on the properties of the guiding region and the multiferroic materials.

2. Linear guided modes

As for the spin dynamics of the localized moments $\mathbf{S}$ in the multiferroic, a classical treatment is appropriate. This is because of the relatively large magnetic moment, finite temperatures, and existing magnetic anisotropies. Furthermore, we are interested in the scattering of waves with wavelengths much larger than the interatomic distance. Therefore, we adopt a continuum model treatment of $\mathbf{S}$. The magnetic ($\mathbf{H}$) and the electric ($\mathbf{E}$) fields are governed by magnetoelectric or chiro-optical Maxwell equations:

$$\frac{\partial \mathbf{S}}{\partial t} = |\gamma| \mu_0 \left[\mathbf{S} \times \mathbf{H} \right], \quad \mu_0 \frac{\partial}{\partial t} [\mathbf{H} + \mathbf{S}] = -\nabla \times \mathbf{E}, \quad \epsilon_0 n_0^2(y) \frac{\partial}{\partial t} \left[\mathbf{E} + c \epsilon_0 n_2 \mathbf{E} |\mathbf{E}|^2 \right] = \nabla \times \mathbf{H}. \tag{2}$$

where γ is the gyromagnetic ratio and μ_0 is the permeability of free space.

The system resides in a stable ground state where the magnetic moments are ordered according to $\mathbf{S}_0 = \mathbf{z} S_{0z}(x) + \mathbf{y} S_{0y}(x)$ in the layer, which we take as the $y-z$ plane. For a moderate amplitude of the incident wave it is sufficient to consider linear field-induced fluctuations $\mathbf{S}_1(x, y)$ around the ground state $\mathbf{S}_0$. The back action of $\mathbf{S}_1$ on the wave propagation determines $\mathbf{H}(x, y)$. Here, we note a key difference to scattering from conventional spin waves which is usually relevant in the GHz regime. In contrast, the spatial modulation of the spin in our case is set by the static spin texture of the ground state $\mathbf{S}_0$ which varies on the scale of tens of nanometers [16]. The wavevector characterizing this helical ordering Q is in our case the same for the upper and lower multiferroic interface (Q is also referred to as the helicity index), meaning we take both the upper and lower boundary regions to be of the same material. Experimental and theoretical studies

Optics EXPRESS

[11,17] evidence that the local spins in the helical oxides are coupled antiferromagnetically (ferromagnetically) along the x-axis (z-axis), as indicated in Fig. 1(a). The helical ordering is along the y-axis. The length scales of the helical and antiferromegnetic order are set by $L = 2\pi/Q$ and h. By applying $\mathbf{E_0}$ along the z-axis, we can tune [15] the helicity index Q.

Following [3,15] one can write the guided mode solution of (2) for the electric field components in the linear approximation $n_2 = 0$ as follows:

$$\mathbf{E} = \frac{1}{2}\mathbf{\Phi}(y)e^{i(\omega t - k_x x)} + c.c., \tag{3}$$

where ω is the linear electromagnetic field frequency and k_x is a propagation constant. $\mathbf{\Phi}(y)$ has a different pattern in different parts of the structure, particularly:

$$\Phi_x = a_x^+ \sin(k_y y), \quad \Phi_y = a_y^+ \cos(k_y y), \quad \Phi_z = a_z^+ \sin(k_y y) \qquad \text{if} \qquad |y|<w/2; \tag{4}$$

$$\Phi_x = b_x^+ e^{-\kappa|y|} \sin(Qy), \quad \Phi_y = b_y^+ e^{-\kappa|y|} \cos(Qy), \quad \Phi_z = b_z^+ e^{-\kappa|y|} \sin(Qy) \quad \text{if} \quad |y|>w/2$$

where $\mathbf{a}^+$ and $\mathbf{b}^+$ are complex amplitudes that will be determined from matching the field components at the interfaces $|y| = w/2$. The wave vector k_y follows from the relation $k_y^2 = \omega^2 n_0^2/c^2 - k_x^2$, while κ characterizes the guided mode confinement and is expressed as:

$$\kappa = \frac{\omega_M^2}{8Qc^2}\left(1 + \frac{c^2 k_x^2}{(n_0'\omega)^2}\right). \tag{5}$$

Its maximal value [15] is reached at:

$$(n_0'\omega)^2 = c^2\left(Q^2 + k_x^2\right). \tag{6}$$

Equation (6) which expresses the dispersion $\omega(k_x)$ of the confined modes, is of key importance to our study. This is because we need to find the linear modes as a first step to construct the weakly nonlinear modes. In (5) we have defined $\omega_M \equiv |\gamma|\mu_0 S_0$.

3. Nonlinear mode derivation

With the propagation modes in the linear regime being identified, the weakly nonlinear solitonic solution can be found by using the well-established reductive perturbation method as detailed in [18,19]. Following this procedure we find the nonlinear envelope soliton solution as a modulation of the linear modes (3) in the following form:

$$\mathbf{E} = \frac{1}{2}\mathbf{\Phi}(y)\Psi(\xi,\tau)e^{i(\omega t - k_x x)} + c.c., \quad \text{where} \quad \xi = \varepsilon(x - vt), \quad \tau = \varepsilon^2 t, \quad v = \frac{\partial\omega}{\partial k_x} \tag{7}$$

where ε is a small expansion parameter and it is supposed that $\Psi \sim \varepsilon$. Then, we apply the multiple scale analysis leading to the nonlinear Schrödinger equation:

$$-i\frac{\partial\Psi}{\partial\tau} + \frac{1}{2}\frac{\partial^2\omega}{\partial k_x^2}\frac{\partial^2\Psi}{\partial\xi^2} + \gamma|\Psi|^2\Psi = 0; \quad \omega'' = \frac{\partial^2\omega}{\partial k_x^2}; \quad \gamma = c\epsilon_0 n_2 \frac{\int_{-w/2}^{w/2} dy\left(\Phi_x^2 + \Phi_y^2 + \Phi_z^2\right)^2}{\int_{-\infty}^{+\infty} dy\left(\Phi_x^2 + \Phi_y^2 + \Phi_z^2\right)} \tag{8}$$

with a one-soliton solution of the nonlinear guided mode:

$$\mathbf{E} = \frac{1}{2}\mathbf{\Phi}(y)\frac{e^{i[(\omega - A^2 N_\Phi/2)t - k_x x]}}{\cosh\left[(x - vt)A\sqrt{N_\Phi/\omega''}\right]} + c.c., \tag{9}$$

Optics EXPRESS

where

$$N_\Phi \equiv \frac{c\epsilon_0 n_2}{A^4}\int_{-w/2}^{w/2} dy\left(\Phi_x^2+\Phi_y^2+\Phi_z^2\right)^2; \qquad A^2 \equiv \int_{-\infty}^{+\infty} dy\left(\Phi_x^2+\Phi_y^2+\Phi_z^2\right); \tag{10}$$

Here, N_Φ is a measure of nonlinearity, A is the soliton amplitude and "c.c." stands for complex conjugate. We note that the nonlinearity causes a modulation of the linear modes along the propagation direction (along the x-axis in Fig. 1), while the transverse profile (along the y-axis) is not modified due to the decaying character inside the multiferroic material. The width of the modulation in (9) is defined as $\Lambda \equiv \sqrt{\omega''/N_\Phi}/A$ is evidently a light intensity dependent quantity. Having determined the electric field of the temporal chiral soliton, we derive similar expressions for the magnetic field components **H** from Maxwell's Eqs. (2). The chirality density pattern is determined according to the relation [20]:

$$\langle\chi\rangle = \frac{\omega}{2c^2}\Im(\mathbf{E}\cdot H^*) \sim 1/\cosh^2\left[(x-vt)A\sqrt{N_\Phi/\omega''}\right] \tag{11}$$

Here, $\Im$ indicates the imaginary part. We note that the chirality density is a quadratic function with respect to the field modulation, as evident from Figs. 1(b) and (c).

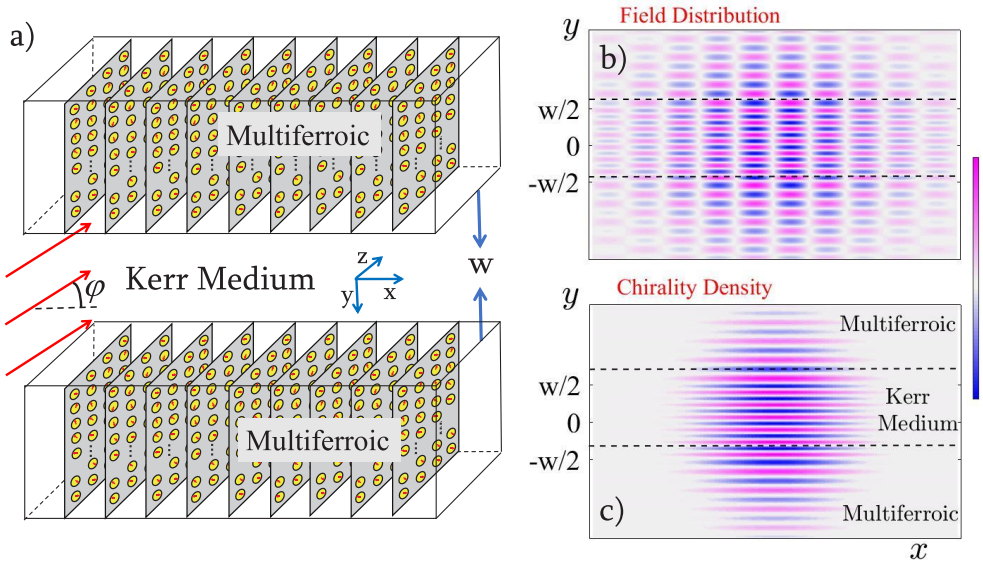

Fig. 1. (a) Schematics of an electrically controlled methodology for purely chiral light enclosed between two chiral multiferroic layers. The thickness of the nonlinear material is referred to as w. The incident angle from the guiding medium is φ. Graphs b) and c) show the distribution of the electric field component E_x and a pattern of the chirality density of the guided mode, respectively. The graphs are plotted according to the soliton profile formula (9) and the expression for the chirality density (11). We use the following parameters: helicity index $Q = \omega_M/2c$, refractive indices $n_0 = 3.4$ (for silicon in the guiding region), $n_0' = 2.4$ (for multiferroic material), and the angle of incidence $\varphi = 75^0$. The length of the multiferroic sample is $400L$, where $L = 10h$.

4. Discussions

From (9) it follows that the nonlinear mode frequency is $\omega_0 \equiv \omega - A^2 N_\Phi/2$ and thus, the frequency of the injected signal should be ω_0 in order to excite the guided mode. From the dispersion

Optics EXPRESS

relation (6) we obtain the following expression:

$$\sqrt{Q^2 + k_x^2}/n_0' - A^2 N_\Phi/2 = \omega_0. \tag{12}$$

We calculate the propagation constant k_x, the soliton velocity $v = \omega' \equiv \partial\omega/\partial k_x$ and the velocity dispersion ω'' knowing the soliton amplitude A, the helicity index Q and light angular frequency ω_0. Then, the incident angle φ impinging from the guiding medium (see Fig. 1(a)) is uniquely defined as follows:

$$\cos\varphi = \frac{ck_x}{\omega n_0} = \frac{n_0' k_x}{n_0\sqrt{Q^2 + k_x^2}}. \tag{13}$$

Particularly, in the linear regime, we consider the scattering problem of waves incoming from the guiding medium on the multiferroic sample and plot in Fig. 2 (main plot) the wave chirality characteristics of reflected waves from the multiferroics when the incident angle is $\varphi = 75^0$. The scattering simulations are performed using our originally developed numerical code based on the rigorous coupled wave method (RCWM). For technical details we refer to the supplemental material in [3]. From Fig. 2 it follows that for the fixed value of the incident angle there exists only a small range of frequencies for which the reflection of the chiral waves takes place. For all other values of ω the waves eventually, taking the Fresnel's reflections, leak out from the multiferroic layers. Changing the values of the incident angles and finding the frequencies ω corresponding to the peak values of the chirality for reflected waves, we can calculate the propagation constant from the formula $ck_x = n_0\omega_0 \cos\varphi$ and consequently, a dependence of k_x versus ω (solid line in the inset of the same Fig. 2). The result of the numerical simulations coincides very well with the analytical formula (6) for the dispersion relation (red circles in the inset) in the whole frequency range. This dispersion relation is used to obtain the spatio-temporal soliton solution. Namely, we find the electric field distribution (see Fig. 1(b)) and the corresponding chirality density of the guided mode (see Fig. 1(c)) following formulas (9) and (11), respectively. Under the prescribed structural parameters, the injected angle φ should be greater than 45^0 in order to avoid an effect of total internal reflection when the incident waves do not "feel" the multiferroic material and no chiral field is formed in the guiding region sandwiched by the multiferroic samples.

To demonstrate the generality of the proposed formalism and in view of experimental realization, we analyze our nonlinear setup in the THz frequency range by examining CS_2 [2] as an optical material enclosed between the multiferroic slabs, i.e., in the guiding region. This material exhibits almost the same nonlinearity characteristics as silicon (Fig. 2) but has smaller linear refractive index which is equal to 1.63. The purpose of employing this optical medium is the following: when using silicon, our setup is realized for a light source embedded in the guiding medium otherwise complete internal reflection occurs because the refractive index of silicon is larger than that of the multiferroic material. For CS_2 as a nonlinear medium, it is possible to use a light source outside the heterostructure (i.e., in free space). Hence, a much larger range of incidence angles can be considered. This is demonstrated in Fig. 3, where the chiral density is shown versus ω/cQ at different angles of incidence that are much smaller than those in Fig. 2.

Finally, it should be emphasized that an important feature of our structure is that the helicity index Q can be controlled by a static applied electric field [3]. For a fixed excitation frequency and keeping the material parameters the same, the normalized propagation constant k_x/k_0 can be uniquely controlled only by an applied electric field. Thus, the proposed structure allows us to flexible control a formation and propagation of the chiral optical soliton.

Optics EXPRESS

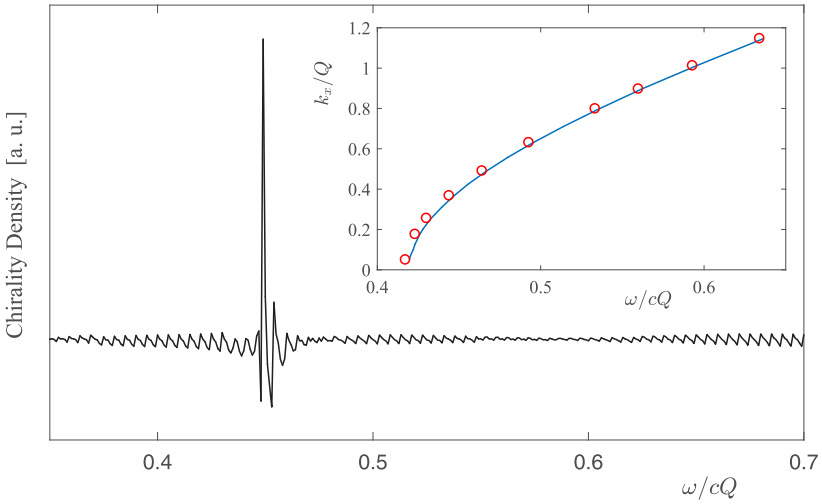

Fig. 2. Main plot: Chirality density (11) of the reflected plane wave scattered from the multiferroic wall at an incident angle $\varphi = 75^0$ impinging from the guiding region. We use a refractive index $n_0' = 2.4$ for the multiferroic material and $n_0 = 3.4$ (silicon) for the guiding medium in our simulations. The inset shows the dispersion curve for the guided mode as calculated from rigorous scattering simulations (solid line) and the analytical formula (6) indicated by the red circles. The scattering simulations are performed using our originally developed numerical code based on the rigorous coupled wave method.

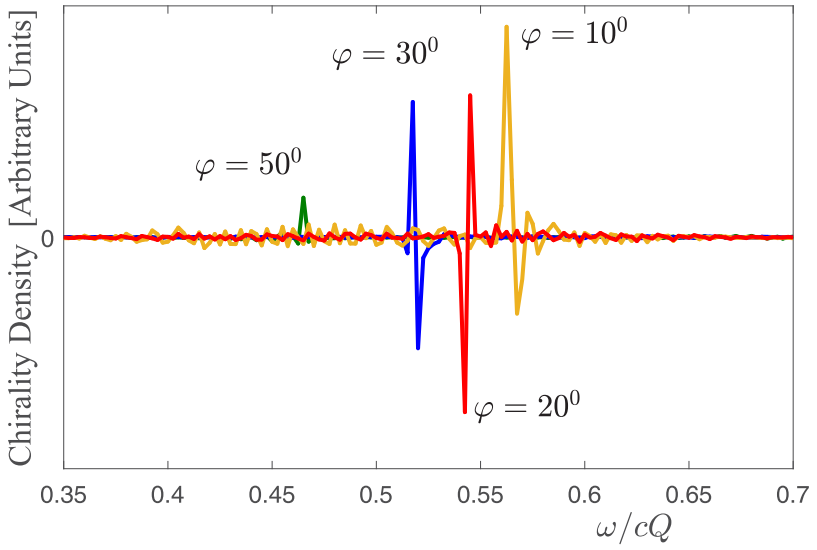

Fig. 3. Chirality density (11) of the reflected plane wave upon scattering from the multiferroic wall at the incident angles $\varphi = 10^0, 20^0, 30^0$ and 50^0 impinging from the guiding region. We use a refractive index $n_0' = 2.4$ for the multiferroic material and $n_0 = 1.63$ (CS_2 [2]) for the guiding medium in our simulations.

Optics EXPRESS

5. Conclusion

We revealed for the first time the possibility of exciting envelope solitons propagating through a guiding medium with Kerr nonlinearity sandwiched between two multiferroic layers with tunable spin topological properties. The soliton is characterized by a nontrivial chirality pattern due to the multiferroic coating. In a next step we plan to extend the numerical simulations as to deal with chiral solitons propagating through a nonlinear cylindrical waveguide with a multiferroic coating, a case of considerable interest for photonic applications.

Funding. Deutsche Forschungsgemeinschaft (287022738, 429194455.).

Acknowledgement. This work has been supported (J.B.) by the Deutsche Forschungsgemeinschaft (DFG) under Project Nr. 429194455. D.E. and V.J. acknowledge the partial support by DFG under Project 287022738 CRC/TRR 196 MARIE (Project M03). Open access is made possible by the publication funds of the Martin-Luther University Halle-Wittenberg.

Disclosures. The authors declare no conflicts of interest.

Data availability. Data underlying the results presented in this paper are not publicly available at this time but may be obtained from the authors upon reasonable request.

References

1. J. Leuthold, C. Koos, and W. Freude, "Nonlinear silicon photonics," Nat. Photonics **4**(8), 535–544 (2010).
2. M. C. Hoffmann, N. C. Brandt, H. Y. Hwang, *et al.*, "Terahertz Kerr effect," Appl. Phys. Lett. **95**(23), 231105 (2009).
3. V. Jandieri, R. Khomeriki, K. Watanabe, *et al.*, "Tunable chiral photonic cavity based on multiferroic layers," Opt. Express **31**(16), 26591 (2023).
4. E. U. Condon, "Theories of optical rotatory power," Rev. Mod. Phys. **9**(4), 432–457 (1937).
5. Y. Tang and A. E. Cohen, "Optical chirality and its interaction with matter," Phys. Rev. Lett. **104**(16), 163901 (2010).
6. C. Genet, "Chiral light–chiral matter interactions: an optical force perspective," ACS Photonics **9**(2), 319–332 (2022).
7. D. Schulz, B. Schwager, and J. Berakdar, "Nanostructured spintronic emitters for polarization-textured and chiral broadband THz fields," ACS Photonics **9**(4), 1248–1255 (2022).
8. J. Zhang, S. Huang, Z. Lin, *et al.*, "Generation of optical chirality patterns with plane waves, evanescent waves and surface plasmon waves," Opt. Express **28**(1), 760 (2020).
9. S.-W. Cheong and M. Mostovoy, "Multiferroics: a magnetic twist for ferroelectricity," Nat. Mater. **6**(1), 13–20 (2007).
10. F. Kagawa, M. Mochizuki, Y. Onose, *et al.*, "Dynamics of multiferroic domain wall in spin-cycloidal ferroelectric $DyMnO_3$," Phys. Rev. Lett. **102**(5), 057604 (2009).
11. M. Fiebig, T. Lottermoser, D. Meier, *et al.*, "The evolution of multiferroics," Nat. Rev. Mater. **1**(8), 16046 (2016).
12. H. Katsura, N. Nagaosa, and A. V. Balatsky, "Spin current and magnetoelectric effect in noncollinear magnets," Phys. Rev. Lett. **95**(5), 057205 (2005).
13. M. Mostovoy, "Ferroelectricity in spiral magnets," Phys. Rev. Lett. **96**(6), 067601 (2006).
14. C. Jia, S. Onoda, N. Nagaosa, *et al.*, "Microscopic theory of spin-polarization coupling in multiferroic transition metal oxides," Phys. Rev. B **76**(14), 144424 (2007).
15. V. Jandieri, R. Khomeriki, L. Chotorlishvili, *et al.*, "Photonic signatures of spin-driven ferroelectricity in multiferroic dielectric oxides," Phys. Rev. Lett. **127**(12), 127601 (2021).
16. R. D. Johnson, L. C. Chapon, D. D. Khalyavin, *et al.*, "Giant improper ferroelectricity in the ferroaxial magnet $CaMn_7O_{12}$," Phys. Rev. Lett. **108**(6), 067201 (2012).
17. L. Ponet, S. Artyukhin, T. Kain, *et al.*, "Topologically protected magnetoelectric switching in a multiferroic," Nature **607**(7917), 81–85 (2022).
18. T. Taniuti, "Reductive perturbation method and far fields of wave equations," Prog. Theor. Phys. Suppl. **55**, 1–35 (1974).
19. J. W. Boyle, S. A. Nikitov, A. D. Boardman, *et al.*, "Nonlinear self-channeling and beam shaping of magnetostatic waves in ferromagnetic films," Phys. Rev. B **53**(18), 12173–12181 (1996).
20. D. L. Andrews, "Fundamental symmetry origins in the chiral interactions of optical vortices," Chirality, 1–15 doi:10.1002/chir.23604 (2023).